Article:

Childs, THC (2018) Comment on 'The cutting of metals by plastic buckling' by Udupa et al. Proceedings of the Royal Society A: Mathematical, Physical and Engineering Sciences, 474 (2216). ISSN: 1364-5021

https://doi.org/10.1098/rspa.2018.0170

Comment on 'The cutting of metals by plastic buckling' by Udupa et al.

Author: T.H.C. Childs*

*School of Mechanical Engineering, University of Leeds, Leeds LS2 9JT, UK

e-mail: t.h.c.childs@leeds.ac.uk

Abstract.

In a recent paper on machining annealed copper at a low cutting speed, and at an uncut chip thickness one tenth of the mean grain size of the copper, Udupa et al. (*Proc. R. Soc A***473**:20160863, doi:10.1098/rspa.2016.0863) report chip thicknesses larger than 10 times the uncut thickness and then a new mode of chip formation. Plastic bulging occurs in the surface of the copper ahead of the tool, leading to chip formation by a series of folds. The strain in the chip is less than that expected in a chip formed by shear according to long-standing classical theory. The authors suggest that the foundations of that theory need to be re-examined. In response, continuum mechanics numerical simulations presented here show a continuous transition from the classical condition towards that observed by Udupa et al. as the ratio of chip thickness to uncut thickness increases above ≈ 7. Bulging is obtained by introducing (approximately) material heterogeneity to the simulations at a grain size scale but whether such heterogeneity is essential for the bulging flows remains an open question.

Key words. Cutting, plasticity, annealed metals, instability, chip formation, finite element modelling.

1. Background

Udupa et al. [1] report observations of a bulging instability in the surface of work material ahead of the chip formation zone in metal cutting. It results in chip formation by a folding flow instead of by the steady shearing that is the basis of long-standing theory. They develop an approximate bifurcation analysis to predict the bulging as a form of buckling and suggest that the foundations of the long-standing theory need to be revisited. This can be taken in two ways: exploring the limits of the long-standing theory, or revisiting models of surface instability. The comments here respond mainly to the first and in a limited way to the second.

The main results in [1] are for machining an annealed copper, of mean grain size 0.5 mm with a tool of rake angle $\gamma = 0°$ and edge radius less than 5 μm, at a cutting speed $v_c = 0.5$ mm/s and uncut chip thickness $h = 0.05$ mm. Subsidiary results are for the same conditions except $\gamma = 45°$, and for machining the copper with the $\gamma = 0°$ tool after applying a pre-strain $\bar{\varepsilon}_p \approx 2.5$. The comments here are made around these conditions. They are based on results from finite element simulations carried out in response to the discussion in [1], though with a tool of edge radius 10 μm (for minimum mesh size reasons), using the bespoke for machining commercial finite element software AdvantEdge-2D, developed from [2], with its option that enables users to include their own material flow stress model. Details are in Appendix A.

2. The limits of long-standing theory.

Simulated chip formations and strain distributions for the conditions in [1] are in figure 1. The much reduced chip thickness caused by pre-straining the work (figure 1b compared to 1a) and the much smoother free surface when $\gamma = 45°$ (figure 1c) follow the observations in [1]. The chip thickness in figure 1a is ≈ 14 times the uncut thickness. Bulging and folding flow is not observed but the extent of plastic strain ahead of the chip and the strain gradient across the chip are significantly larger than in figures 1b and c.

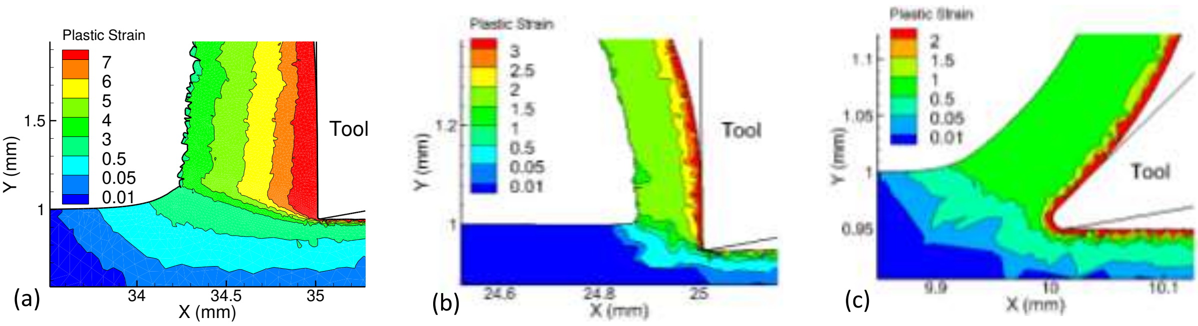

Figure 1. Predicted chip formations, with strain contours: (a) $\bar{\varepsilon}_p = 0$, $\gamma = 0°$, (b) $\bar{\varepsilon}_p = 2.5$, $\gamma = 0°$, (c) $\bar{\varepsilon}_p = 0$, $\gamma = 45°$.

Long standing theory in its most basic form, rigorously applicable only to non-strain hardening metals and straight chips, considers a chip of thickness t to be formed from the uncut thickness h by shear across a flat plane inclined at the shear plane angle ϕ to v_c. It is a standard result that ϕ, t/h and γ are linked geometrically (equation 1), and that the equivalent strain in the chip due to the shear, $\bar{\varepsilon}_{shear}$, depends on ϕ and γ (equation 2).

$$\tan\phi = \cos\gamma / (t/h - \sin\gamma) \tag{1}$$

$$\bar{\varepsilon}_{shear} = \left(1/\sqrt{3}\right)\cos\gamma / \left[\sin\phi\cos(\phi-\gamma)\right] \tag{2}$$

Real chip formations are more complicated but t/h can still be measured and an equivalent ϕ and $\bar{\varepsilon}_{shear}$ calculated. The actual mean strain $\bar{\varepsilon}_{simulation}$ in a simulated chip can be found by averaging across the chip thickness. This includes the secondary shear strain next to the tool, not accounted for in equation 2. Thus $\bar{\varepsilon}_{simulation}/\bar{\varepsilon}_{shear} > 1.0$ is expected for a chip formed in simple shear. In fact, for the case of figure 1a the ratio $\bar{\varepsilon}_{simulation}/\bar{\varepsilon}_{shear}$ is 0.64, less than 1 and also similar to that in [1].

Simulations, with $\gamma = 0°$ and $\bar{\varepsilon}_p$ from 0 to 3, and with $\bar{\varepsilon}_p = 0$ and γ from 0° to 45° show that $\bar{\varepsilon}_{simulation}/\bar{\varepsilon}_{shear}$ reduces below 1.0 by > 10% for t/h greater than ≈ 7 (figure 2a). The example of figure 2b ($\bar{\varepsilon}_p = 0$, $\gamma = 0°$) demonstrates that the reduction is due to compression ahead of the shear zone. Material approaching the shear zone is compressed two- to three-fold before shearing. From the strain rate contours the highest strain rates in the shear zone occur along a plane inclined to v_c at ≈ 1.5 times the angle from t/h (equation 1). The final strain is then the sum of a compression ≈ ln2.5 and a shear ≈ 2/3rd of that from equation 2.

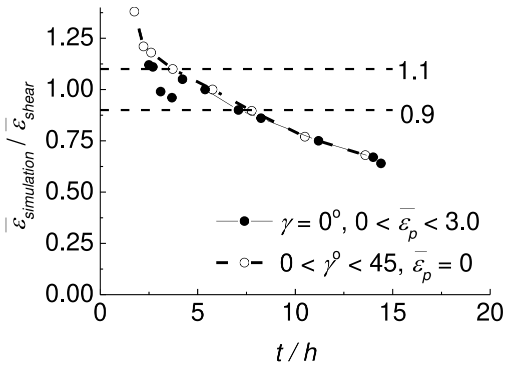

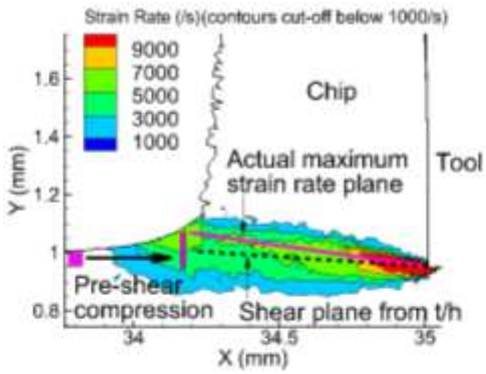

Figure 2. (a) the dependence of $\bar{\varepsilon}_{simulation}/\bar{\varepsilon}_{shear}$ on t/h; (b) pre-shear compression, example of $\bar{\varepsilon}_p = 0$, $\gamma = 0°$, to explain $\bar{\varepsilon}_{simulation}/\bar{\varepsilon}_{shear} < 0.9$ for $t/h > 7$. ($\bar{\varepsilon}_{simulation}/\bar{\varepsilon}_{shear} > 1.1$ for $t/h < 2$ is due to including the large secondary shear strains next to the rake face (figure 1) in $\bar{\varepsilon}_{simulation}$.)

The separation in figure 2b between the actual maximum strain rate plane and that from equation 1 is another aspect of the departure of chip formation from simple shear. For *t*/*h* less than ≈ 7 there is no separation (as is classically observed and as is the basis of many successful analyses of chip formation [3]). Beyond that, with increasing *t*/*h*, pre-compression increasingly modifies chip formation, towards the extreme form observed in [1].

3. Surface instabilities.

Figure 3a shows the chip formation when $\bar{\varepsilon}_p = 0$, $\gamma = 0°$, at greater magnification than in figure 1a. Strain contours are cut-off above 4 to concentrate on the pre-shear and chip surface regions. The pre-shear free surface deforms steadily, concave upwards with no bulging. Surface instability occurs at the exit to the shear region. In this case bulging ahead of the shear region requires heterogeneity to be introduced. The software is able to simulate this in a limited way, by modelling the work piece as two slabs separated by a slice of some other material. Figure 3b shows chip formation when a softer slice has just entered the pre-shear region. It is 0.5 mm wide to match the grain size in [1], is initially parallel-sided and its flow stress is 80% of that to either side (see Appendix A). The free surface ahead of the chip is now convex upward with an incipient bulge, with shear split into major and minor bands.[1]

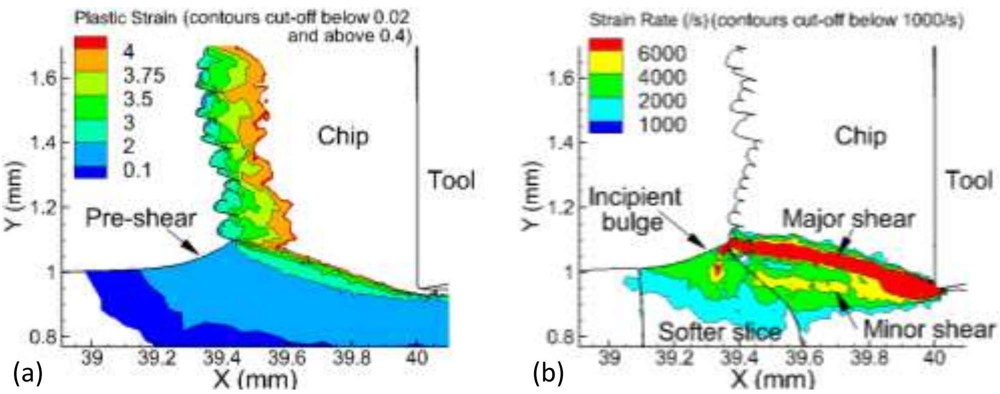

Figure 3. (a) strain contours (b) strain rate contours, with (a) no surface bulge in the pre-shear zone, and (b) an incipient bulge forming as a softer slice enters the pre-shear zone.

The strain rate field in figure 3b is similar to that in wedge compression under traction [4]. The bulge would develop by squeezing between the two shear regions and folding would follow from transfer of shear severity between the bands as the work steadily approaches the

[1] The software's limitation is that the slab/slice interfaces do not transmit shear, only compressive normal stresses. It is not possible realistically to follow the growth of the bulge as the slice moves towards the major shear band. But at the early stage of figure 3b shear stresses are naturally low across the interfaces, as judged by the near-continuity of the strain rate contours. The limitation is then not so distorting of the flow.

tool. It gives a deterministic explanation of bulging, alternative to buckling, that is not considered in [1] despite split and oscillating shear zones having been previously reported in machining brass, albeit on a finer scale, in figure 12 of [5] and the ghost of a similar field having been reported for sinuous flow in figure 2 of [6]. Publication of the strain rate fields from the streak lines in [1] would be valuable. Further, although heterogeneity is responsible for bulging in figure 3b, it is possible to imagine the same mechanism occurring in more severe (larger t/h) conditions without the need for that. In contrast, prior work with a softer slice in the manner of figure 3b shows that heterogeneity is necessary in the less severe condition of plastic wave flow under a sliding wedge [7]. The role of heterogeneity merits further study.

4. Final comments.

This comment's simulations show a continuously changing mode of chip formation as t/h increases from ≈ 7 to 14: shear gives way to pre-compression and shear but the bulging and folding state seen in [1] is not reached. Bulging, with more the appearance of wedge compression under traction than buckling, occurs at large t/h when local softening is introduced, to represent the effect of grain-scale heterogeneity but in this condition, due to a software limitation, it has not been possible to continue the simulations to what might become a folding flow. In this comment's view whether [1]'s bulging has a bifurcation or a more deterministic explanation, and whether heterogeneity is essential for its occurrence remain open questions.

Competing interests. The author has no competing interests.
Acknowledgement. The author is grateful to Professor S. Chandrasekar (co-author of [1]) for making available additional information and for constructive discussions during preparation of these comments.
Funding. These comments are unfunded.

Appendix A. The model details

A Johnson-Cook flow stress model is applied, omitting temperature and strain rate terms, as in [1] because of the low cutting speed condition that is being modelled, but with two modifications from its usually presented form (equation A1): pre-strain is accommodated by introducing the variable $\bar{\varepsilon}_p$; a saturation strain $\bar{\varepsilon}_c$ is introduced above which strain hardening ceases. With this temperature and time independent flow stress model simulation results are independent of cutting speed. v_c = 100 m/min is chosen as the elapsed computing time is hugely reduced compared to that for v_c = 0.5 mm/s.

$$\begin{aligned}\bar{\sigma} &= A + B\left(\bar{\varepsilon}_p + \bar{\varepsilon}\right)^n, \quad \left(\bar{\varepsilon}_p + \bar{\varepsilon}\right) \le \bar{\varepsilon}_c \\ &= A + B\bar{\varepsilon}_c^{\,n} \qquad\quad , \quad \left(\bar{\varepsilon}_p + \bar{\varepsilon}\right) > \bar{\varepsilon}_c\end{aligned} \tag{A1}$$

The software's plane strain sliding friction model is applied (equation A2), with τ_f the friction stress and σ_n the normal stress between chip and tool and μ the friction coefficient.

$$\tau_f = \min(\bar{\sigma}/\sqrt{3}, \mu\sigma_n) \tag{A2}$$

Selecting A = 90 MPa, B = 290 MPa and n = 0.31, as referenced in [1], with $\bar{\varepsilon}_c$ in the range 3 to 3.5 and μ from 0.3 to 0.35, gives predicted chip thickness to uncut chip thickness ratios and forces similar to those in [1]. $\bar{\varepsilon}_c$ = 3.4 and μ = 0.33 are chosen for the results in Sections 2 and 3. A = 72 MPa and B = 235 MPa are chosen for the softer slice in figure 3b.

References

1. Udupa A, Viswanathan K, Ho Y, Chandrasekar S. 2017 The cutting of metals via plastic buckling. *Proc. R. Soc. A***473**, 20160863. (doi:10.1098/rspa.2016.08630)

2. Marusich T, Ortiz M. 1995 Modelling and simulation of high speed machining. *Int. J. Numer. Methods Eng.* **38**, 3675-3694. (doi:10.1002/nme.1620382108)

3. Oxley PLB. 1989 *Mechanics of machining*. Chichester, UK: Ellis Horwood Ltd., Chs. 5-7.

4. Johnson KL. 1968 Deformation of a plastic wedge by a rigid die under the action of a tangential force. *J. Mech. Phys. Solids* **16**, 395-402. (doi:10.1016/0022-5096(68)90003-3)

5. Guo Y, Compton WD, Chandrasekar S. 2015 *In situ* analysis of flow dynamics and deformation fields in cutting and sliding of metals. *Proc. R. Soc. A***471**, 20150194. (doi:10.1098/rspa.2015.0194)

6. Yeung H, Koushik V, Compton WD, Chandrasekar S. 2015 Sinuous flow in metals. *Proc. Natl. Acad. Sci. USA* **112**, 9828-9832. (doi:10.1073/pnas.1509165112)

7. Vandana AS, Sundaram K. 2017 Interaction of a sliding wedge with a metallic substrate containing a single inhomogeneity. *Tribol. Lett.* 65:124. (doi:10.1007/s11249-017-0910-0)